EFFECT OF FLUIDIZED BED ON PERMEATE FLUX IN CERAMIC MEMBRANE CROSS-FLOW MICROFILTRATION

Petr MIKULASEK

Department of Chemical Engineering,
University of Pardubice, 532 10 Pardubice, Czech Republic

Received November 18, 1994
Accepted August 28, 1995

The microfiltration of a model fluid on an α-alumina microfiltration tubular membrane in the presence of a fluidized bed has been examined. Following the description of the basic characteristic of alumina tubular membranes, model dispersion and spherical particles used, some comments on the experimental system and experimental results for different microfiltration systems are presented. From the analysis of experimental results it may be concluded that the use of turbulence-promoting agents resulted in a significant increase of permeate flux through the membrane. It was found out that the optimum porosity of fluidized bed for which the maximum values of permeate flux were reached is approximately 0.8.

Membrane filtration processes are currently mostly used in the production of ultrapure water, the processing of food and dairy products, the recovery of electrodeposition paints, the treatment of oil and latex dispersions and in biotechnology oriented applications. However, the present membrane processes for liquid feed streams are complicated by the phenomena of membrane fouling and of concentration polarization in the liquid boundary layer adjacent to the membrane wall. Concentration polarization (CP) and membrane fouling are major concerns for the successful use of membrane-based separation operation in a cross-flow mode, as their net effect is to reduce the permeate flux, thereby resulting in less productivity. Such limitations have spurred on the research to the development of new membrane materials and the utilization of novel hydrodynamic approaches in membrane separation systems.

The use of inorganic membranes in separation technologies is relatively new and has given rise to much of interest in recent years. The main group of ceramics used in ceramic-membrane manufacturing are the refractory oxides: alumina, zirconia and titania. Ceramic membranes exhibit unique physical and chemical properties which are only partially developed (or are completely absent) with polymeric membranes. For example, ceramics can be used at significantly higher temperatures, have better structural stability without the problems of swelling or compacting, can usually withstand harsher chemical environments, are not subjected to microbiological attack, and can be backflushed, steam sterilized or autoclaved. Ceramic membranes represent a distinct

class of inorganic membranes. Other classes include membrane materials such as glasses, carbon and metals, and organic–inorganic polymers[1].

Of the various methods mentioned in ref.[2], hydrodynamic or fluid management techniques have proved to be quite effective and economical in reducing CP and fouling. Each of these methods has achieved a certain success in practice. For example, it was reported that membrane systems with fluidized bed in retentate have successfully been used for liquid food processing (see refs[3–6]).

The fluidized bed concept needs to operate with tubular membrane modules in vertical position. The principle of intensifying mass transfer and significant reducing CP is mainly based on the effect on the membrane wall caused by the collision of fluidized particles (polymer, metal or glass balls). This interaction reduces, in comparison with the empty tube experiments, the thickness of the boundary layer and increases the mass transfer coefficient[4,6–8].

In a recent paper[9], more specially concerned with cross-flow microfiltration of latex waste water on alumina membranes, we have demonstrated that a limiting flux was observed which depended on the types of latexes and on the flow velocity of the feed. The decrease in the flux of permeate was attributed to the resistance of the cake (gel) layer formed on the membrane or blocking the pores in the membrane. Owing to these obstacles, low permeate fluxes resulted at relatively high solution velocity.

The present study, which represents a continuation of that work, was undertaken with a view to get a better insight into the basic transport mechanisms which take place at the wall of membranes from movements of free agents in the presence of a fluidized bed.

EXPERIMENTAL

Membranes

The ceramic membranes studied in this work were asymmetric, double-layered, alumina membranes (Terronic, Czech Republic). They were configured as single cylindrical tubes 0.2 m long, 12 mm ID and 17 mm OD, consisting of a thin α-alumina layer deposited on the internal surface of the tubular alumina support. In our experiments, the microfiltration membranes were used with the mean pore diameter equal to 0.2 μm. The pore size distribution of the membrane used (see Fig. 1) was determined by the liquid displacement method[10]. The data presented in Fig. 1 indicate that the double-layer ceramic membrane used in these studies has a very narrow pore-size distribution. This narrow distribution is extremely useful for accurate predicting the performance of tubular ceramic membranes in different applications.

Feeds

Two different fluids were used either with the empty tube or the fluidized bed system to determine the effect on flux. The first one was prefiltered deionized water, and the second one was the diluted dispersion of an alumina powder in deionized water. The particle size distribution of the alumina

powder used, shown in Fig. 1, was determined by a particle sizer SediGraph 5100 (Micromeritics). Concentration of solids in the dispersion was constant (1% w/w).

Equipment

The microfiltration studies were carried out in a membrane filtration unit equipped with ceramic membranes. The unit contained two identical modules: one with fluidized bed in retentate and second with an empty membrane. The fluids were circulated through the module by a centrifugal pump. The unit allowed studies in which the transmembrane pressure and the cross-flow velocity were independently varied.

A schematic diagram of the experimental apparatus is shown in Fig. 2. It consisted mainly of microfiltration modules 1, a pump 2, a storage tank 3 equipped with a thermal regulation system 4, and a temperature and pressure control system.

Experiments were carried out at 25 °C, either with (fluidized bed experiments) or without (empty tube experiments) particles. The liquid was fed into the bottom of the vertical membrane at a constant volumetric flow rate regulated with control valves located at the pump outlet. The supports of the membrane consisted of two stainless steel meshes compressed between rubber packing. A calming section of 2 mm diameter spheres was placed immediately below the support.

At first, the flow of prefiltered deionized water through the membrane was examined under various transmembrane pressures (i.e., the dif-

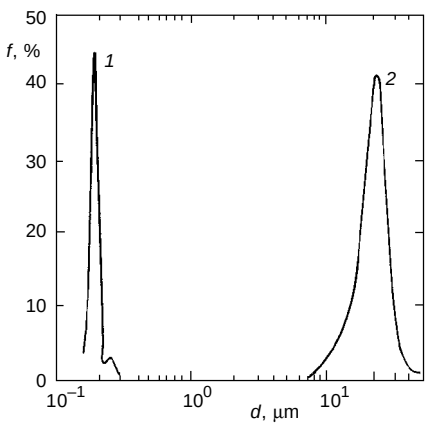

FIG. 1
Pore size distribution of 0.2 μm membrane (*1*) and particle size distribution of Al_2O_3 dispersion used (*2*)

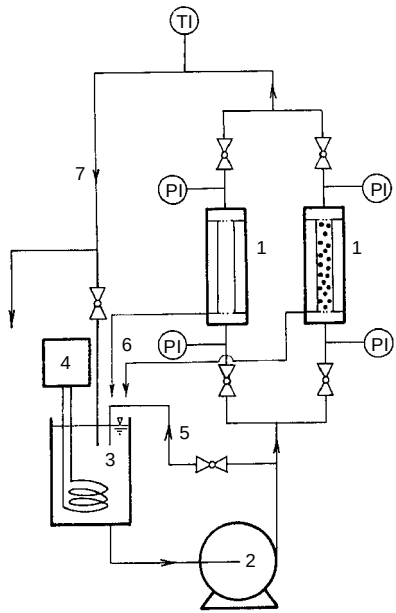

FIG. 2
Scheme of experimental apparatus: 1 microfiltration modules (left-hand with an empty membrane, right-hand with fluidized bed in retentate); 2 pump; 3 storage tank; 4 thermal regulating system; 5 by-pass; 6 permeate stream; 7 retentate stream

ference between values of the pressures measured by means of two pressure gauges PI and permeate outlet pressure – see Fig. 2) in the range 0–150 kPa while the superficial velocity was fixed at a constant value. (It is worth recalling that superficial velocity, u, is defined in both the systems as the ratio of volumetric flow rate to membrane tube cross-sectional area.) Then, the alumina powder dispersion was measured at a constant transmembrane pressure ΔP = 50 kPa. For various superficial velocities in the range 0.03–0.28 m s^{-1}, the permeate flux, J, was evaluated. The contribution to the transmembrane pressure drop due to the fluid flow through the fluidized bed resulted in a pressure drop of 2 kPa. Thus, at a total transmembrane pressure of 50 kPa, the pressure drop attributable to the fluidized bed was only 5%, hence the fluidized bed pressure drop was assumed to be negligible for all calculations. A new membrane was used in each experiment, and before the run, the pure water flux through the membrane was measured. The dispersion was then introduced to the unit, the pump was powered on and operating pressure and superficial velocity adjusted by the regulation system. The flux through the membrane was measured by collecting the permeate from the outer Perspex tube surrounding the membrane into graduated cylinder and timing the collection period. Both the permeate and the retentate were recycled to the storage tank to maintain a relatively constant dispersion concentration. Every experiment was carried out until the flux became actually constant.

Fluidized particles were either glass beads of 1.46 mm diameter and 2 506 kg m^{-3} density or stainless steel beads of 1.00 mm diameter and 7 506 kg m^{-3} density. For each experiment with fluidized bed, the column was filled with solids in such a way that the total expanded bed height was equal to membrane length. The corresponding solid loading (for the glass beads 5.7–22.7 . 10^{-3} kg, for the steel beads equal to 17.0–68.0 . 10^{-3} kg) and superficial velocities were known from the preliminary results on hydrodynamics obtained in a transparent tube with the same diameter as the membrane.

RESULTS AND DISCUSSION

Pure Water Flow

An important parameter when determining membrane retention characteristics (the ability of a membrane to hinder a component to pass through it or to retain a component in the fluid) is the mean pore diameter of microfiltration membranes having a narrow pore-size distribution (see Fig. 1). In general, the smaller the pore diameter, the higher will be the rejection coefficient of particulates/solutes of a greater nominal size. However, as the pore size decreases, the permeability of liquid also rapidly decreases[11]. The typical pure water (prefiltered deionized water) fluxes, as a function of the transmembrane pressure, are shown in Fig. 3 for different experiments. As evident from this figure, the flux for deionized water rises linearly with transmembrane pressure according to the flux equation

$$J = \frac{\Delta P}{\mu R_m} \quad , \tag{1}$$

where R_m is the hydraulic resistance of the membrane. The hydraulic resistance R_m is a membrane property and does not depend on the feed composition or on the transmembrane pressure ΔP. From the slopes of plots of J versus ΔP, given in Fig. 3, the hy-

draulic resistances for the empty tube experiments, $R_{me} = 4.19 \cdot 10^{11}$ m^{-1}, and for the fluidized bed experiments (glass particles were used), $R_{mf} = 4.30 \cdot 10^{11}$ m^{-1} may be estimated. As expected, it can be seen that the value of the ratio R_{me}/R_{mf} is close to unity. However, on the contrary, the absolute value of hydraulic resistance of membrane was higher for the fluidized bed experiment, probably due to the higher dispersion variance of experimental values. Thus, these observations do not confirm results of empty tube and fluidized bed experiments presented by Rios et al.[6]. The observed difference between the values of R_{me} and R_{mf} ($R_{me}/R_{mf} \approx 4$) reported in ref.[6] is explained by the existence of the ordered water structure elements near the membrane surface, which are minimized by increasing turbulence. However, the conclusion mentioned in the paper[6] cannot be simply related to the absorbent properties of alumina membranes only. Our explanation of the results presented by Rios et al.[6] is based on the differences in the water quality for testing their systems. In accordance with the well-known effect of water purity on water flux[12], the membrane fouling by bacteria and trace colloids in the empty tube system may be suggested. In this hypothesis, the membrane fouling could be reduced in the presence of a fluidized bed.

Microfiltration of the Alumina Dispersion

Analysis of the permeate composition showed complete retention of the alumina particles in the feed. Note that the diameter of the dispersion particles was always much larger than the membrane pore size (see Fig. 1) in order to prevent particle penetration into or through the membrane.

Values of the permeate flux versus time for various mean feed velocities in the empty tube system are plotted in Fig. 4 for the alumina dispersion used. As a general rule, the steady-state flux during cross-flow microfiltration was substantially lower than

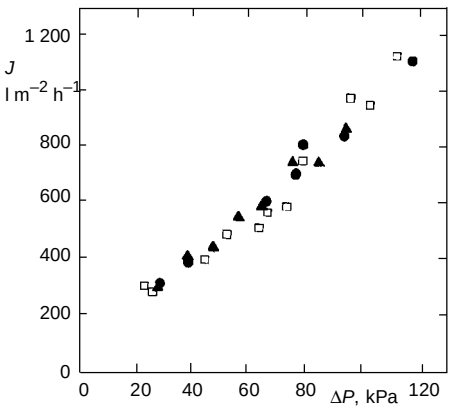

FIG. 3
Permeate fluxes of pure water in dependence on transmembrane pressure: ❐ empty tube experiments; ● fluidized bed experiments (glass beads, $\varepsilon = 0.7$); ▲ fluidized bed experiments (glass beads, $\varepsilon = 0.8$)

the pure water flux – ranging from 30% to 95% of the pure water values. Besides the fact that high levels of permeate flux are achievable (for comparison see ref.[9]), the most noticeable feature in Fig. 4 is the strong dependence of the flux on the superficial velocity of the feed. The following trends are evident:

a) A significant flux decay was observed mainly in the initial periods of the process, and

b) the flux decline shows significant dependence on operating conditions such as superficial velocity.

The flux decay in the initial periods of process could be explained by build-up of CP and/or the formation of a cake layer on the membrane surface which offers the controlling hydraulic resistance to permeation. Steady-state conditions as a result of CP are reached when the convective transport of particles to the membrane is equal to the sum of the permeate flow plus the diffusive back transport of the particle. (It should be remembered that only CP phenomena are considered here with fouling being excluded.) In addition, for very low superficial velocity, the filter cake continues to grow until it reaches a state where further growth is curtailed by the applied axial fluid shear upon the filter cake. At this point, steady-state flux should be reached. It is evident from Fig. 4 that this steady-state flux increases (the thickness of the cake layer and its hydraulic resistance decreases) with the superficial velocity.

Experiments with the empty ceramic tube module were carried out at superficial velocities resulting in Reynolds numbers Re = 450–3 800, defined as $Re = Du\rho/\mu$. Generally, the flow of Newtonian fluids in circular tubes with nonporous walls is laminar when the Reynolds number is less than 2 300. The behaviour of fluid flow in a porous channel is different than that in a nonporous-wall channel. In case of cross-flow microfiltration, the flow may be close to the transition between laminar and turbulent

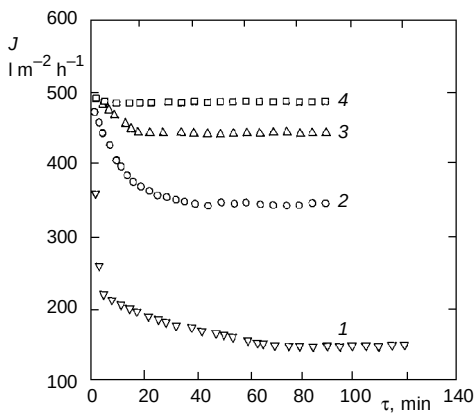

FIG. 4
Permeate flux vs time for alumina dispersion microfiltration – empty tube experiments (ΔP = 50 kPa): *1* u = 0.05 m s^{-1}; *2* u = 0.10 m s^{-1}; *3* u = 0.20 m s^{-1}; *4* u = 0.28 m s^{-1}

when the Reynolds number changes from 2 300 to nearly 6 000 depending on the module geometry, superficial velocity and permeate flux through the membrane.

Figure 5 illustrates the effect of the superficial velocity on the steady-state permeate flux, J_{ss}, for the alumina dispersion sample. An increase in superficial velocity from 0.05 to 0.28 m s^{-1} resulted in a permeate flux increase by a factor of about 3 under otherwise equal operating conditions. The slope of the plot $J_{ss}(u)$ for superficial velocity in the range from 0.10 to 0.28 m s^{-1} is 0.34 which is very close to the one-third power dependence of a system operating under laminar conditions and predicted by the Brownian diffusion mechanism of concentration polarization[13]. This result indicates that none of the back-transport (shear-induced back diffusion or inertial lift) or surface-transport mechanism[14] could at present be considered dominant for the changes in filtration rate.

The values of permeate fluxes versus time show in the course of microfiltration in the presence of fluidized particles the same shape of $J(\tau)$ curves (Fig. 6) compared to those of the empty tube experiment (see Fig. 4). However, a strong and non-monotonous dependence of permeate flux at steady-state, J_{ss}, upon the superficial fluid velocity and/or porosity may be observed. As a rule, the values of the steady-state permeate flux in the fluidized bed system are superior to the ones obtained in the empty tube, with a maximum ratio of 1.5 (Fig. 7). On the whole, these results agree well with scattered information on the intensification of microfiltration by a fluidized bed already publish-

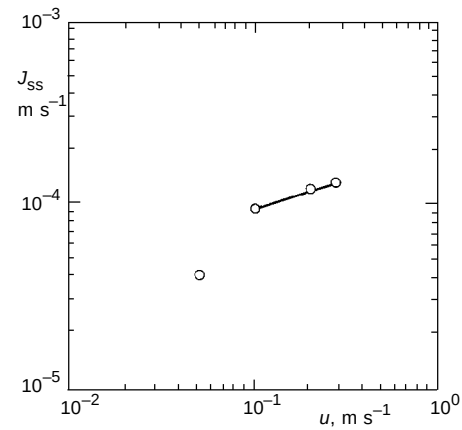

FIG. 5
Variation of steady-state permeate fluxes with superficial velocity for alumina dispersion microfiltration (ΔP = 50 kPa)

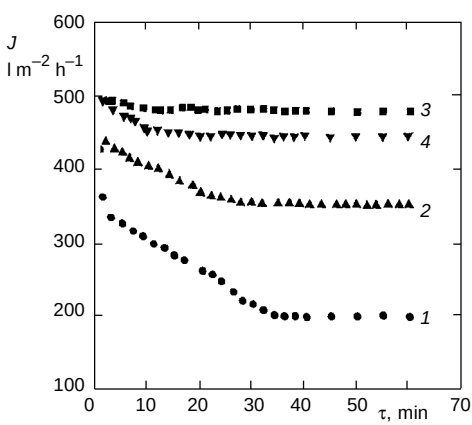

FIG. 6
Permeate flux vs time for alumina dispersion microfiltration – fluidized bed experiments (glass beads, ΔP = 50 kPa): *1* u = 0.025 m s^{-1}; *2* u = 0.053 m s^{-1}; *3* u = 0.113 m s^{-1}; *4* u = 0.155 m s^{-1}

ed in literature[5,6,8]. Fluidized particles act as obstacles to the fluid flow in the same way as if they were fixed within a membrane; because of their presence, turbulence is increased and CP is weaker and/or cake layers are considerably thinner than in the empty tube. However, particle motion may be thought of as being responsible for strong and continuous erosion of particle deposits at the wall. The number of collision of the particles per unit membrane area per unit of time is proportional to bed porosity[4]. Particle-cake contacts are certainly more effective than turbulence when ε is varied in the interval around the value of 0.8 (see Fig. 8), when slugging of a fluidized bed was observed in the course of preliminary experiments on hydrodynamics obtained in a transparent tube.

A more extensive study of the effect of a shear rate on permeate flux was made in studies comparing the steady-state flux of empty tube and fluidized bed systems. The results show that an operational run time of approximately 1 h produces a reasonable flux where it may be assumed that the plateau corresponding to the steady-state flux value is reached. To facilitate comparison between the two different systems considered, the shear rate at the inner membrane surface, assuming Newtonian fluid behaviour of the alumina dispersion and fully-developed laminar flow, was approximated for the cross-flow tube system by Eq. (*2*)

$$\dot{\gamma}_w = 8u/D \qquad (2)$$

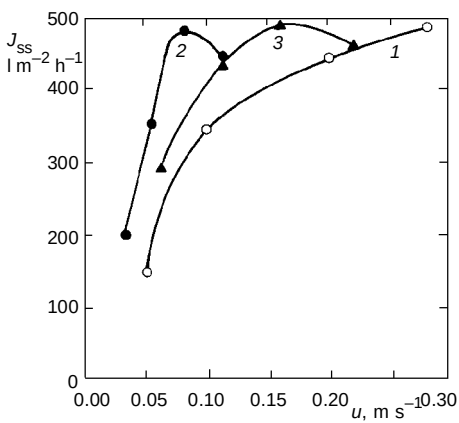

FIG. 7

Variation of steady-state permeate fluxes with superficial velocity for alumina dispersion microfiltration (Δ*P* = 50 kPa): *1* empty tube experiments; *2* fluidized bed experiments (glass beads); *3* fluidized bed experiments (stainless steel beads)

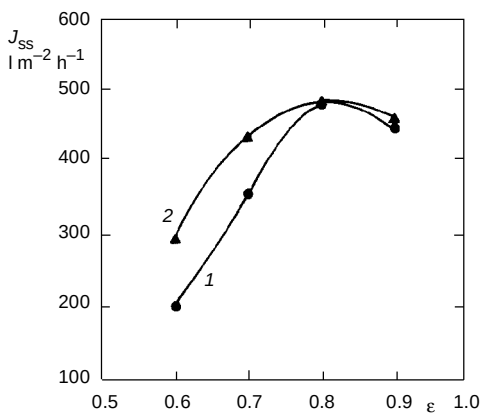

FIG. 8

Variation of steady-state permeate fluxes with fluidized bed porosity for alumina dispersion microfiltration (Δ*P* = 50 kPa): *1* glass beads; *2* stainless steel beads

and for fluidized bed system by the relation[15]

$$\dot{\gamma}_w = 12u(1 - \varepsilon)/\varepsilon^2 d_p \qquad (3)$$

substituting the corresponding experimental values of superficial velocity u and bed porosity ε, respectively.

As shown in Fig. 9, the steady-state permeate flux in the fluidized bed system was non-monotonous one with estimated shear rate at the membrane inner wall as well. It is evident that the flux had not reached a maximum at the lower shear rate ($\dot{\gamma}_w$ = 115 s^{-1}), corresponding to the maximum experimental value of superficial velocity (u = 0.155 m s^{-1}) and bed porosity (ε = 0.9), respectively. On the contrary, the flux in the empty tube system was nearly linear with increasing shear rate above the value of approximately 30 s^{-1} at the membrane surface.

It follows from Fig. 9, that the steady-state permeate flux in empty tube and fluidized bed systems was approximately the same for the value of the shear rate close to 180 s^{-1}. On the other hand, this value of the steady-state permeate flux (approximately 480 l m^{-2} h^{-1}) was obtained in the empty tube system using the superficial velocity 3.5 times higher that observed in the fluidized bed system.

CONCLUSIONS

The use of turbulence-promoting fluidized particles resulted in a significant increase of permeate flux through the membrane. However, it has been noticed that the flux reaches a maximum for the optimum bed porosity in dependence on the superficial velocity of the feed.

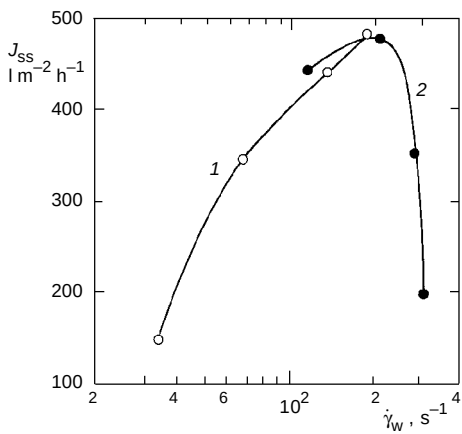

FIG. 9
Variation of steady-state permeate flux with wall shear rate for alumina dispersion microfiltration (ΔP = 50 kPa): *1* empty tube experiments; *2* fluidized bed experiments (glass beads)

From the analysis of hydraulic resistances, it may be concluded that fluidized solids insure a significant reduction of the concentration polarization and membrane fouling, as well as a continuous mechanical erosion of the particle deposits at the wall of the membrane. In this case, the improved permeate flux that is achieved is due to the combined action of turbulence and particle motion (collision of particles with membrane wall). This reduces the thickness of the surface boundary layer and also reduces the hydraulic resistance of CP and/or a cake layer.

These attractive properties of the fluidized bed (a significant modification of CP, and a strong erosion of the particle layer on the membrane wall) may be used to advantage, for example, in the design of new bioreactors or separators.

SYMBOLS

d	diameter of membrane pore or alumina particle, m
d_p	diameter of fluidized particles, m
D	inner diameter of the membrane tube, m
f	frequency, %
J	permeate flux, l m^{-2} h^{-1}
ΔP	transmembrane pressure, Pa
R_m	hydraulic membrane resistance, m^{-1}
$Re = Du\rho/\mu$	Reynolds number
u	superficial velocity of feed, m s^{-1}
$\dot{\gamma}_\omega$	shear rate at wall, Eqs (*2*) and (*3*), s^{-1}
ε	bed porosity
μ	dynamic viscosity of liquid, Pa s
ρ	density of liquid, kg m^{-3}
τ	time, s
Subscript	
e	refers to empty tube
f	refers to fluidized bed
ss	refers to steady-state

The described research work was financially supported by the Grant Agency of the Czech Republic (Grant No. 104/93/2306).

REFERENCES

1. Bhave R. R.: *Inorganic Membranes.* Van Nostrand Reinhold, New York 1991.
2. Mikulasek P.: Collect. Czech. Chem. Commun. *59*, 737 (1994).
3. van der Waal M. J., van der Velden P. M., Konig J., Smolders C. A., van Swaay W. P. M.: Desalination *22*, 465 (1977).
4. De Boer R., Zomerman J. J., Hiddink J., Aufderheyde J., van Swaay W. P. M., Smolders C. A.: J. Food Sci. *45*, 1522 (1980).
5. Montlahuc G., Tarodo de la Fuente B., Rios G. M.: Entropie *124*, 24 (1985).
6. Rios G. M., Rakotoarisoa H., Tarodo de la Fuente B.: J. Membr. Sci. *34*, 331 (1987).

7. Xuesong W.: Desalination *62*, 211 (1987).
8. Clavaguera F., Rjimati E., Elmaleh S., Grasmick A.: Key Eng. Mater. *61–62*, 569 (1991).
9. Mikulasek P., Cakl J.: Desalination *95*, 211 (1994).
10. Mikulasek P., Dolecek P.: Sep. Sci. Technol. *29*, 1183 (1994).
11. Mikulasek P., Dolecek P., Seda H., Cakl J.: Dev. Chem. Eng. Miner. Process. *2*, 115 (1994).
12. Fane A. G., Fell C. J. D.: Desalination *62*, 117 (1987).
13. Ho W. S. W., Sirkar K. K.: *Membrane Handbook*. Van Nostrand Reinhold, New York 1992.
14. Belfort G., Davis R. H., Zydney A. L.: J. Membr. Sci. *96*, 1 (1994).
15. Machac I., Mikulasek P., Ulbrichova I.: Chem. Eng. Sci. *48*, 2109 (1993).